

WiSER-X: Wireless Signals-based Efficient Decentralized Multi-Robot Exploration without Explicit Information Exchange

Ninad Jadhav, Meghna Behari, Robert J. Wood, and Stephanie Gil

Abstract—We introduce a Wireless Signal based Efficient multi-Robot eXploration (WiSER-X) algorithm applicable to a decentralized team of robots exploring an unknown environment with communication bandwidth constraints. WiSER-X relies only on local inter-robot relative position estimates, that can be obtained by exchanging *signal pings* from onboard sensors such as WiFi, Ultra-Wide Band, amongst others, to inform the exploration decisions of individual robots to minimize redundant coverage overlaps. Furthermore, WiSER-X also enables asynchronous termination without requiring a shared map between the robots. It also adapts to heterogeneous robot behaviors and even complete failures in unknown environment while ensuring complete coverage. Simulations show that WiSER-X leads to 58% lower overlap than a zero-information-sharing baseline algorithm-1 and only 23% more overlap than a full-information-sharing algorithm baseline algorithm-2.

I. INTRODUCTION

Coordinated decentralized multi-robot exploration of an unknown environment is relevant for many applications such as search-and-rescue as it enables faster exploration and avoids single points of failure [1]. Efficient exploration of the environment traditionally requires information exchange between the coordinating robots. Often it includes local map estimates, common features or landmarks, and relative position estimates. However, such information exchange is often limited by communication bandwidth constraints, non-line-of-sight conditions, remote operations, or on-board computation limitations on robots with size, weight and power constraints. For instance, robots in a search-and-rescue mission may lack line-of-sight, or underwater gliders may operate without GPS and high-bandwidth communication.

Existing works have made significant progress to address these limitations by developing methods such as (1) using prior centralized information to pre-assign robots to regions of the environment before deployment [2] (2) sharing post-processed data like sparse environmental features to estimate common coverage areas [3], or (3) requiring periodic rendezvous [4], such as surfacing to communicate or obtain GPS fixes during underwater exploration [5]. While these approaches have enabled significant progress towards coordinated exploration in challenging environments, they come with limitations such as precluding real-time adaptation to heterogeneous robot performance and failures, and/or extending mission times by requiring rendezvous. In an ideal setting, robots could assess each other’s coverage in real-time *without* explicit communication, reducing redundancy in exploration

while eliminating interruptions or high bandwidth information exchanges. Additionally, the algorithm would adapt to heterogeneous behaviors, for example, assigning larger portions of the environment to be explored by robots with better navigation capabilities.

Along these lines, we introduce WiSER-X, a decentralized coordination algorithm that allows robots to improve their local frontier exploration strategy by leveraging onboard relative Angle-of-Arrival (AOA) and range measurements to other robots in the team (Fig 1). AOA and range can be measured in a variety of settings, including acoustically in underwater environments [6], and using RF signals (such as WiFi and Ultra Wide-band) in indoor environments for example. Importantly, communication pings needed to measure AOA and range between robots are much more lightweight, typically requiring 32 kb/s as opposed to 2.5 Mb/s for full feature map exchange, and can traverse longer distances through NLOS occlusions.

We address the following key challenges when developing WiSER-X. As choosing a frontier to visit depends on its utility [7], we update the information gain of robots’ frontiers by estimating potential overlaps, computed based on the estimated relative position of neighboring robots obtained from range and bearing sensor measurements. As such, once a robots’ local frontier’s utility falls below a certain threshold, it is marked as invalid and no longer a candidate during the current timestep. However, robots still need to know when to terminate exploration without a shared map. To address this, robots’ maintain a history of the relative positions locally in a hgrid data structure, enabling them to track which robots have visited various areas within the environments boundary (known apriori). Thus a robot terminates exploration asynchronously when there are no valid frontiers left or when it independently estimates that the environment has been sufficiently covered. WiSER-X also adapts to to heterogeneity in robot behavior or even complete failures in real-time, minimizing the exploration time without loss of coverage in comparison to the baseline algorithms.

To accurately estimate positions from noisy AOA and range measurements from real sensors, we use an Extended Kalman Filter (EKF) to maintain accurate relative positioning, even in environments with potential multipath interference. WiSER-X also adjusts the weight of a neighboring robot’s information overlap at a frontier based on the certainty of their relative position estimates. WiSER-X thus enables efficient, coordinated decentralized multi-robot exploration using only AOA and range measurements acquired from ping packets at 32 kb/s. We validate our method through extensive simulations and hardware experiments, showing (1)

*Authors are affiliated with the School of Engineering and Applied Sciences, Harvard University, Cambridge, MA 02138, USA. We gratefully acknowledge partial funding support through Project CETI and NSF CAREER grant CNS-2114733. We thank Hammad Izhar for his support on designing the sensor mounts.

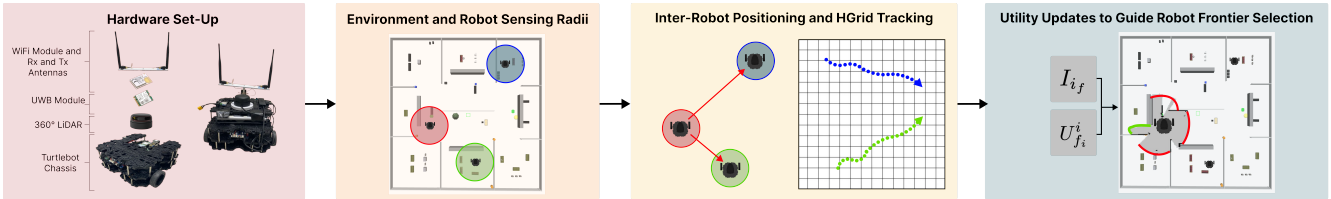


Fig. 1: From left to right, the first panel shows the hardware components used for onboard sensing. The second panel visualizes the environment with each robot’s sensing radius within it. The third panel shows how a robot can leverage both inter-robot positioning and historical exploration to infer which parts of the environment have been explored. Finally, the last panel shows how this information is used to update the utilities of the frontiers for a given robot, and it uses this to guide its exploration.

improvements in time to completion, (2) reduced coverage overlap, (3) minimized missed areas in exploration, and (4) effective handling heterogeneity in robot behaviors.

II. RELATED WORK

Several strategies have been proposed to improve exploration of an unknown environment with a single robot or a team of robots [8]–[14]. However, decentralized multi-robot exploration in unknown environments predominantly requires significant data exchange such as map updates, sensor data, trajectories or positions in common frame of reference [15]. Reducing communication exchange is a significant area of study and much of the research in this area focuses on minimizing such *explicit* data exchange [16]–[18] using methods such as compressing map data before transmission to reduce communication load, reducing the number of robots involved in communication [19], limiting data exchange to when robots are in close proximity [20], [21], and designating a subset of robots as connectivity robots that are responsible for maintaining network links [22]. Intermittent rendezvous, where robots plan periodic meetings to share information throughout a mission, is another common technique [23]–[25]. However, all of these methods rely on some baseline form of information transmission which are prone to multiple issues such as perceptual aliasing and not always possible in communication bandwidth constrained environments. Thus, despite these developments in reducing communication load via *explicit* information exchange for multi-robot tasks, there is still limited research on fully decentralized exploration methods that leverage low-bandwidth *implicit* information exchange to increase efficiency in exploration. While methods do discuss updating individual robots’ belief states to guide their exploration strategies [26]–[28], they often still depend on non-trivial levels of communication or a centralized “auction” system [29].

To circumvent such constraints, some methods aim to reduce communication overhead through *implicit* information exchange. This approach typically involves integrating optical cues or relative position estimates into each robot’s task strategy to minimize redundancy. [30], [31] use optical wireless communication for multi-robot position coordination, while [32], [33] use IR or UV LEDs for robot identification and position estimation. However, these methods require consistent line-of-sight.

Another critical aspect of decentralized multi-robot exploration is the ability for robot teams to adapt to the heterogeneous conditions of individual agents, such as varying robot

dynamics (e.g., navigation speed or sensing capabilities) or failures within the collective mission. As a result, methods that pre-assign exploration regions to each robot [34], [35] lack the flexibility to adapt in completely unknown environments due to reliance on prior information such as the internal structure or knowledge of obstacles. On the other hand, many existing approaches to handling robotic failures or heterogeneity still rely on centralized systems [26], [36], [37] or require periodic explicit communication between robots [38], [39]. While [40] addresses dynamic decentralized demand coverage using only relative positions of robots, it does not explicitly explore low-cost methods for obtaining these positions.

Our method addresses these challenges in the literature by utilizing onboard sensing that utilizes *ping packets* to locally obtain relative position estimates of other robots. The adoption of onboard wireless signal based sensing for robotics has increased tremendously in the last few years [41]–[50]. Additionally, research has explored fusing such sensors to develop more accurate systems for relative pose estimation, even in communication-constrained environments [32], [51]–[53]. We show that the integration of such local relative position estimates into a decentralized frontier-based exploration framework leads to efficient exploration with minimal redundancy without the need to exchange any other information between the robots. Our algorithm also enhances the system’s robustness, enabling it to handle robotic failures and heterogeneity in performance effectively.

III. PROBLEM

We consider a team $\mathcal{R} \subset \mathbb{R}^{1 \times n}$ of n homogeneous mobile robots exploring an unknown, bounded 2D environment with known dimensions of its outer boundary. Each robot $i \in \mathcal{R}$ is equipped with a finite-range 360° laser sensor, with scan radius r , to map the geometric structure of the environment, represented as a 2D occupancy grid map $\mathcal{M} \subset \mathbb{R}^2$.

The robots operate in a decentralized manner without access to a shared or prior map, and, due to bandwidth constraints, they cannot rely on real-time inter-robot communication of data such as map updates or motion plans. Moreover, the robot team does not use real-time localization methods, as that would require additional data exchange and synchronization.

Each robot relies solely on the information collected from its onboard sensors and maintains a local coordinate frame. Robots independent use global and local path planners to navigate while avoiding collisions. Our goal is to achieve

coordinated exploration of the environment using only local capabilities, relying on inter-robot relative range and bearing estimates derived from lightweight signal exchanges (e.g. “ping packets”). Thus any robot $i \in \mathcal{R}$ can obtain relative measurements to all other robots in its neighborhood $\mathcal{N}_i = \{j | j \in \mathcal{R}, j \neq i\}$.

For exploration, each robot uses a frontier-based exploration algorithm. Given a local map \mathcal{M}_i of robot i , a frontier $f_i \subset \mathbb{R}^{n \times 2}$ consists of k grid cells that are on the boundary of the known and unknown space in \mathcal{M}_i . \mathbf{F}_i denotes the set of all such frontiers generated by robot i at time t . Robots compute a scalar *utility* value of all frontiers $f_i \in \mathbf{F}_i$ based on (1) information gain $\mathcal{I}_i^{f_i}$, defined as the number of unexplored cells within radius r from the center of a frontier, and (2) the navigation cost $\mathcal{C}_i^{f_i}$, defined as the path length between the robot’s current position and the center of a frontier. Following the approach in [54], the utility $U_i^{f_i}$ of a frontier $f_i \in \mathbf{F}_i$ is then obtained by $\mathcal{I}_i^{f_i} / \mathcal{C}_i^{f_i}$. Thus, the first problem that we need to address to enable efficient distributed multi-robot exploration is as follows:

Problem 1. *Given the communication bandwidth constraints and availability of only locally computed inter-robot measurements for a robot i , develop a frontier-based algorithm such that at every timestep $t \in \{0 \dots \mathcal{T}\}$, where \mathcal{T} denotes total exploration duration, robot i navigates to a frontier f_i that has highest utility and minimal overlap of its map with the explored region of other robot $j \in \mathcal{N}_i$*

$$\hat{f}_i = \arg \max_{f_i \in \mathbf{F}_i} (U_{f_i}^i) \quad (1)$$

We assume that an overlap occurs when robot j ’s relative position at any timestep is within the laser sensor range of robot i ’s frontier.

In order to ensure sufficient exploration of the environment, it is important that all robots successfully map a portion of it before terminating exploration. However, a situation may arise leading to heterogeneity in robot behaviors. We specifically look at two heterogeneous behaviors in the team - i) varying speed of robots during exploration that can result from navigation challenges, and ii) complete failure of a robot leading to loss of its map data. We summarize this in the following problem:

Problem 2. *Under heterogeneous robot behaviors or failures, the robot team should be capable of adapting to the situation such that the exploration of the environment is minimally impacted.*

The robot team eventually stops exploration when there are no more frontiers left. However, given the lack of a shared map between the robots, a robot i does not have a direct estimate of how much of the environment has been collectively explored by the team at any given timestep. This information is critical for terminating exploration and to prevent every robot from exploring the entire environment. Thus, the third problem that we need to address can be stated as follows:

Problem 3. *Each robot i in the team needs to asynchronously determine when to terminate exploration, using only its local information, by estimating total coverage of the environment.*

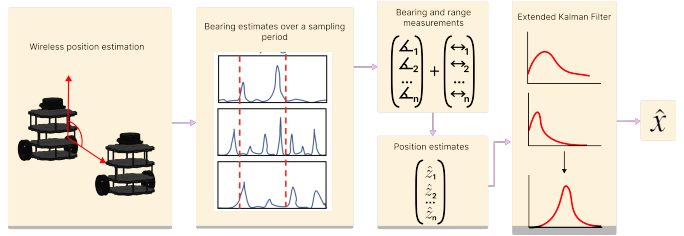


Fig. 2: Position estimation pipeline. Robot i combines the bearing and range measurements to robot j , sampled over a duration of 10 seconds (See Alg. 1). The estimates are iteratively refined using an Extended Kalman Filter to get the best position estimate of robot j .

The last problem that we address is to show the applicability of our algorithm on real robots by obtaining relative inter-robot positions using onboard sensors.

Problem 4. *Robot i needs to estimate relative positions \hat{x}_j for all robots $j \in \mathcal{N}_i$ by integrating range measurement *dist* and bearing measurement φ obtained from onboard wireless signal based sensors. Additionally, \hat{x}_j should be attainable even in presence of signal multipaths.*

In the following section we explain our solution to each of the above problems and develop a system that can be deployed on real robots.

IV. APPROACH

Our goal was to enable a team of robots to explore an unknown environment efficiently through implicit coordination. To achieve this goal, each robot $i \in \mathcal{R}$ used onboard Simultaneous Localization and Mapping (SLAM) algorithm to create a local map \mathcal{M} with a set of frontiers \mathbf{F}_i at every timestep t . Robot i also leveraged the relative positions of nearby robots in their neighborhood \mathcal{N}_i to update the information gain for each frontier and using the hgrid for efficient storage and retrieval of these estimates (Sec IV-A). Robots thus navigated to their local frontiers with the highest utility, while handling heterogeneity in behavior such as complete failures (Sec IV-B), repeating this process until all frontiers are explored or a termination condition is met (Sec IV-C). (Sec IV-D) provides details on how robots obtain relative position estimates using onboard sensing and computation to enable deployment of our algorithm on real hardware.

A. WiSER-X Algorithm

WiSER-X used a frontier-exploration based approach (Algorithm 1), where a robot i calculated the utility $U_{f_i}^i$ of each local frontier f_i based on the estimated position \hat{x}_j of all neighboring robots $j \in \mathcal{N}_i$. Very large frontiers, greater than LiDAR sensor range r , were split into smaller segments along its principle axis obtained using Principal Component Analysis method [55]. It is known that certain directions – “viewpoints” – from a frontier can yield better information than others [55]. Hence, to improve frontier selection, WiSER-X computed the utility at three distinct viewpoints on the frontier corresponding to its center and the two extremes. For simplicity of notation, in the remainder of the paper we denote a robot i ’s frontier’s viewpoint as $x_{f_i}^i$.

Algorithm 1 Frontier Exploration Algorithm

Require:

Local frontier set \mathbf{F}_i of robot i
 Bearing measurements ϕ (from WSR Toolbox)
 Distance measurements D (from UWB sensor)

```

while Selecting Next Frontier do                                ▷ Step 1
   $\varphi \leftarrow \text{StableBearingAngle}(\phi)$ 
   $\hat{\mathcal{M}}_j(\mathbf{t}) \leftarrow [\text{AverageDist}(D), \varphi]$                                 ▷ Step 2
   $\hat{x}_j \leftarrow \text{EKF}(\hat{\mathcal{M}}_j(\mathbf{t}))$ 
  InsertInHgrid( $\hat{x}_j$ )
  for  $f_i \in \mathbf{F}_i$  do                                          ▷ Step 3
     $\mathcal{I}_i^{f_i} \leftarrow \text{Information Gain}(\text{Eqn: 4, 7})$ 
    if Soft Threshold AND  $E(\hat{D}_{jc})/S(D_{fc}) > 0.9$  then
      Remove  $f_i$  from  $\mathbf{F}_i$ 
    else
       $\mathcal{C}_i^f \leftarrow \|x_c^f - x_i\|$ 
       $U_{f_i}^i = \arg \max_{x_v^f} (\beta I_{f_i} / C_f)$  (Eqn:2)
    end if
  end for
  Terminate exploration if  $|\mathbf{F}_i| == 0$  OR Hard Threshold
else
  Next frontier  $\hat{f}_i = \arg \max_{f_i \in \mathbf{F}_i} (U_{f_i}^{f_i})$ 
end while

```

Thus, $U_{f_i}^i$ for f_i was computed as follows -

$$U_{f_i}^i = \arg \max_{x_v^f} (\beta I_{f_i} / C_f) \quad (2)$$

$C_f = \|x_{f_i} - x_i\|_2$ denotes the navigation cost, or the Euclidean distance from the robot's current position x_i to the frontier center x_{f_i} . The navigation cost was not computed separately for each viewpoint as the difference is trivial. The β parameter scaled the overall information gain based on a viewpoint x_v^f 's proximity to the nearest neighboring robot j and was obtained as follows-

$$\beta = \log_{10}(\min_x (\|x_v^f - x_j\|_2)) \quad (3)$$

Thus, β ensured that the when j is very close to a frontier f_i , the information is scaled down substantially. Robot i then chose a frontier with max utility as per equation (1).

We note that robots generated new frontiers continuously at a sufficiently high rate. In order to avoid oscillatory behavior because of this, where a robot might move back-and-forth between two frontiers of similar utility, WiSER-X ensured that the robot committed to its chosen frontier till its half-way to it (based on the path length). Only then it reevaluated the utility of all frontiers generated in the current timestep and changed the target frontier if required.

1) *Information Gain Calculation:* A robot's local map is represented as a gridmap. For any frontier f_i , let E_f be the set of unexplored gridcells c around f_i that are reachable by the robot's sensor range r . The distance $D_{fc} = \|x_v^f - x_c\|^2$ defines how far a gridcell c is from the frontier's viewpoint x_v^f . The information gain I_{f_i} for a frontier f_i in \mathbf{F}_i was calculated by summing the contributions from each gridcell c in E_f . Each cell's contribution was computed based on two factors: (i) proximity to the robot $S(D_{fc})$, a sigmoid function used to prioritize cells closer to the robot, reducing the

information gain for cells farther way, and (ii) overlap with neighboring robots $E(\hat{D}_{jc})$, an information loss term that accounts for areas likely already explored by neighboring robots. Thus, the overall information gain I_{i_f} for f_i was obtained as follows:

$$I_{i_f} = \sum_{c \in E_f} \max(0, S(D_{fc}) - E(\hat{D}_{jc})) \quad (4)$$

where the sigmoid function modulates the information gain based on D_{fc} , prioritizing cells near the robot:

$$S(D_{fc}) = \frac{1}{1 + e^{(D_{fc} - \kappa_1)/\kappa_2}} \quad (5)$$

Here, κ_1 controls the midpoint and κ_2 controls the steepness of the curve, favoring closer cells but permitting distant cells to contribute as well [56]. The max function in equation (4) ensured that the information gain per gridcell was non-negative and lower bounded to 0.

2) *Information Loss Calculation:* We estimated the information loss $E(\hat{D}_{jc})$ for each gridcell by considering neighboring robots' coverage. For each neighboring robot j , an information loss is computed using its estimated positions \hat{x}_j , representing areas it may have already explored. The information loss $E(\hat{D}_{jc})$ was obtained as follows-

$$E(\hat{D}_{jc}) = \sum_{\hat{x}_j \in \hat{X}_j} \min(1, 1/\text{Tr}[\Sigma(\hat{x}_j)]) \cdot S(\hat{D}_{jc}) \quad (6)$$

$S(\hat{D}_{jc})$ is the sigmoid function applied to $\hat{D}_{jc} = \|\hat{x}_j - x_c\|$, while $\min(1, 1/\text{Tr}[\Sigma(\hat{x}_j)])$ scaled it using the trace of covariance Σ for the estimate \hat{x}_j . Thus, equation (6) computed the overlap around f_i based on the accuracy of position estimate of the neighboring robots.

3) *Hgrid operations:* Robot i stored its own position x_i , the estimated position of neighboring robots \hat{x}_j , and the trace of the covariance matrix $\text{Tr}[\Sigma(\hat{x}_j)]$, which represents the uncertainty in the estimated position of neighboring robots. These observations were collected over the duration of exploration and stored in the hgrid, a discretized representation of the environment. The hgrid has a structure similar to a quadtree where each hgrid cell has dimensions equivalent to the sensor radius (see Fig 1). We used this structure to enable fast retrieval of information in $O(\log N)$ time.

Each hgrid cell maintained a count of how many times it had been visited by other robots, which represented a local record of coverage. When deciding which frontier to visit next, robot i queried the hgrid to determine if any neighboring robots were within the sensor range r of a given frontier (See Fig. 1). This enabled choosing frontiers that were less frequently visited by other robots, minimizing redundant coverage. An hgrid-cell is then marked as *filled* once a user-defined threshold of observations was reached, indicating that the area had been sufficiently covered.

B. Adapting to heterogeneous behaviors of robots

We considered two heterogeneous behaviors for the robots. The first scenario involved variability in mapping speed where some robots explored the environment faster than

others. Basically this emulated a situation where, given an unknown environment, some robots may end up in locations that make navigation more challenging. WiSER-X automatically addressed this issue by directing the faster robots to cover more area, compensating for the reduced performance of the slow robots.

The second scenario simulated complete failure of a robot, resulting in the loss of access to its local map for the areas it had covered. This necessitates that the rest of the robots in the team re-explore the areas covered by the failed robot to ensure complete coverage of the environment. We enabled this by updating equation (6) as follows -

$$E(\hat{D}_{jc}) = \sum_{\hat{x}_j \in \hat{X}_j} \tau_j \cdot \min(1, 1/\text{Tr}[\Sigma(\hat{x}_j)]) \cdot S(\hat{D}_{jc}) \quad (7)$$

where $\tau_j \in [0, 1]$ is a binary variable that indicates whether robot j has completely malfunctioned (0) or is functional (1). We assume that when a robot j malfunctions robot i can no longer obtain ping packets from it and thus sets $\tau_j = 0$. As τ_j is maintained as a pointer for all relative positions \hat{x}_j , this operation is executed in $O(1)$. As such, when the robot i computed set of frontiers \mathbf{F}_i in the next timestep, it disregarded all possible overlaps of the failed robot j which allowed for "re-exploration" of the areas j had visited.

C. Exploration termination

As the robot team's collective coverage of the environment increased, the information gain of a robot i 's frontiers gradually decreased. Using its hgrid, robot i continuously updated its coverage estimation. WiSER-X triggered two different termination behaviors by setting two threshold limits, soft and hard, on the hgrid's occupancy, with the former being less than the latter.

When the occupancy reached the soft threshold, robot i disregarded *invalid* frontiers, defined as those for which percentage ratio of information loss (Eqn. 7) to that of information gain (without considering any overlaps, obtained by setting $E(\hat{D}_{jc}) = 0$ in equation 4) is greater than 90%. Robot i terminated exploration asynchronously if no valid frontiers were generated in the current timestep. Once the hard threshold is reached, a robot stops exploration. This can be used to force early termination and could be useful in time-critical applications where full coverage is not necessary. We note that once robots exit the environment, they can merge their local maps by leveraging high-bandwidth communication.

D. Obtaining Relative Positions using onboard sensing and computation

To estimate the relative position \hat{x}_i for a robot $j \in \mathcal{N}_i$, robot i fuses data from its single onboard UWB sensor and the WSR toolbox [41] that used WiFi signal phase. However, obtaining bearing using the toolbox requires emulating a "virtual antenna array" that leverages robot motion [44]. Although previous work has shown that bearing can be achieved by leveraging arbitrary motion of a robot, it requires exchange of data between the signal transmitting and receiving robot [42]. Hence, WSR toolbox collected the relative

signal phase data using a set of two receiving antennas connected to a WiFi card [57] which enabled "passive" bearing estimation. To emulate a virtual antenna array, the setup was deployed on a servo that rotated back-and-forth and obtain a bearing measurement within five seconds. However, due to the multipath phenomenon, the signal can sometimes appear to arrive from several different locations, introducing errors. Robot i used the the WSR toolbox to collect multiple bearing observations $\varphi \in \phi$ for a robot j over a short sampling period. These measurements were then compared to identify those with minimal variation, as multipath-induced bearings fluctuate randomly, while bearings from direct paths remain stable [58]. During the same sampling period, the UWB sensor provided multiple range measurements. A uniform sub-sample of these ranges was taken, and then averaged. By pairing a stable bearing with the average range measurement, robot i generated a preliminary position estimate $\hat{m}_j(t) = [\text{average}(D), \phi]$. Finally, we refined this noisy position estimate using an Extended Kalman Filter (EKF) to produce $\hat{x}_j(t)$, a smoothed position estimate at time t . Figure 2 shows the entire position estimation pipeline can be viewed in .

Thus, by leveraging inter-robot relative position estimates, our exploration algorithm enabled improved coordination during exploration without requiring explicit information exchange.

V. RESULTS

We validated WiSER-X through extensive simulation and hardware experiments and compared its performance against three baseline algorithms.

A. Setup

1) Comparison baselines:

- **Baseline-1: Independent Exploration:** A frontier-based exploration algorithm based on the explore-lite package [59]. In this baseline, each robot ran the explore package on-board and selected frontiers solely based on utility, without considering the locations of other robots. This represents a zero-information-sharing exploration strategy.
- **Baseline-2: Full Information Exchange:** A global frontier-based algorithm using the Rapidly-Exploring Random Tree (RRT)-exploration package [60]. This package employs the RRT [61], incrementally building a tree from a starting point by randomly sampling points in the space and expanding the tree towards those points, favoring high-utility goal points. A global "assigner" node allocated frontiers to robots as an oracle system, representing a full-information-sharing exploration strategy.
- **Baseline-3: Divide-and-Conquer:** Each robot was assigned a specific area to map and concluded its exploration once that area was completely explored. This baseline was only used for evaluating heterogeneous robot behaviors.

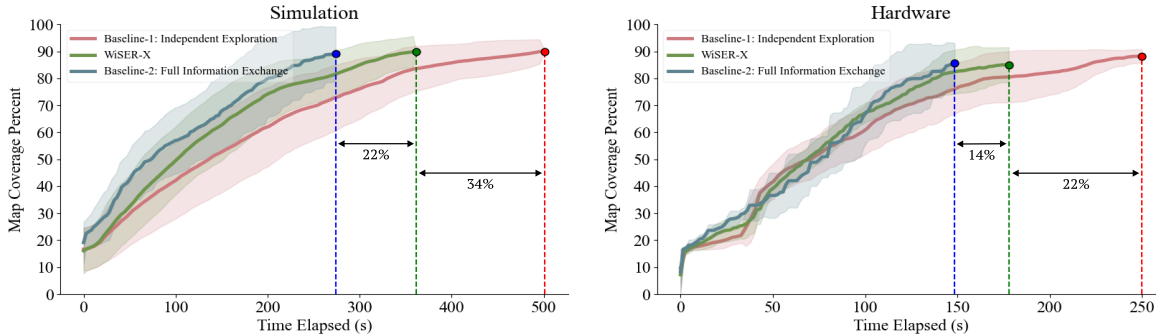
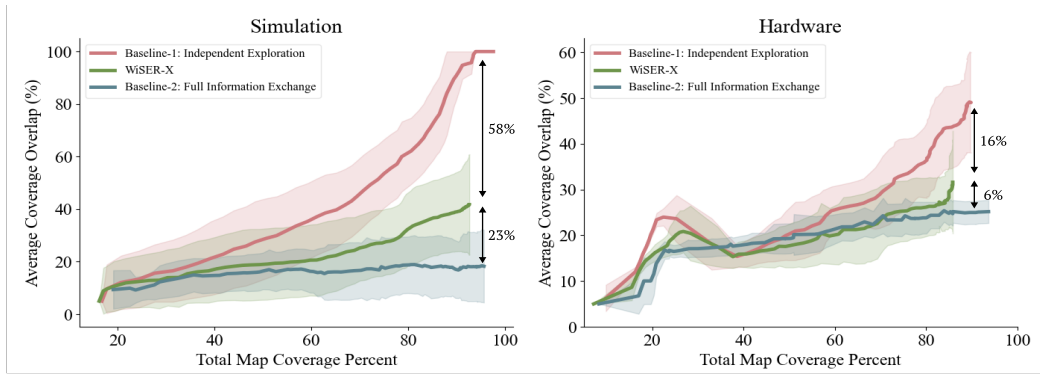


Fig. 3: On the top is average map coverage overlap for each algorithm in both hardware and simulation. On the bottom, the average time elapsed to achieve full map coverage. For the baseline algorithms, termination occurred when the merged map reached 95% coverage. In the WSR algorithm, termination was automatically triggered when each robot determined that global coverage had reached 95%.

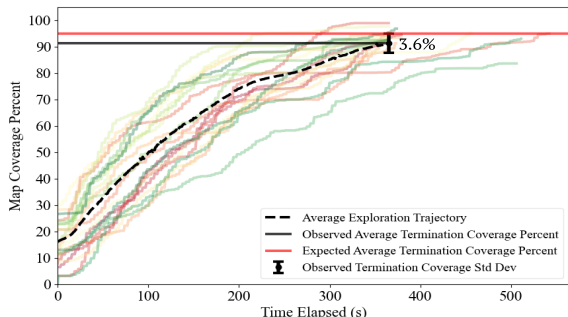


Fig. 4: Map coverage percent for WiSER-X over 20 trials of simulation, with the average performance shown in black.

2) *Environment:* We ran our simulations in the ROS-compatible physics-based simulator Gazebo. We used a 1600 m^2 cluttered office environment (see Fig. 1), with three ground robots, each equipped with an on-board LiDAR. We initialized each robot at random locations throughout the environment over twenty runs for each evaluation scenario. For the WiSER-X algorithm in simulation, we used true positions of the robots combined with simulated noise to generate noisy range and AOA estimates that would be otherwise be obtained from on-board sensors.

We ran real hardware experiments, in a 64 m^2 environment with obstacles (Fig 1). We use two Turtlebot Waffle robots with an on-board LiDAR. Range and AOA measurements were obtained using Qorovo DWM1001-DEV UWB module and WiFi based WSR toolbox respectively. The robots were

initialized at two different positions and we ran three trials for each to compare coverage overlap and exploration duration across all the algorithms. Both simulation and hardware experiments used GMapping SLAM algorithm [62] with SBPL planner.

B. Evaluation metrics

The performance of our algorithm and the baselines is evaluated using a global map-merging ROS package [59]. For the two baseline systems, this map-merging oracle was used for termination, enacted at approximately 95% completion of the environment exploration. WiSER-X, however, performed termination independently by each robot without this central server involvement, as described in IV-C. We evaluated the performance of our algorithm using the following metrics:

- **Coverage overlap:** The overlap between individual robot maps was measured to evaluate the system’s effectiveness in reducing redundancy.
- **Termination time:** The evaluation focused on how quickly and consistently the system could self-terminate the exploration within a set time frame.
- **Heterogeneity in robot behavior:** The system’s robustness was tested by simulating scenarios pertaining to variability in the system (e.g., complete failure and constrained navigation) and comparing the algorithms’ adaptability to them.
- **Impact of sensor noise:** The system’s performance was evaluated under conditions of noise impacting range

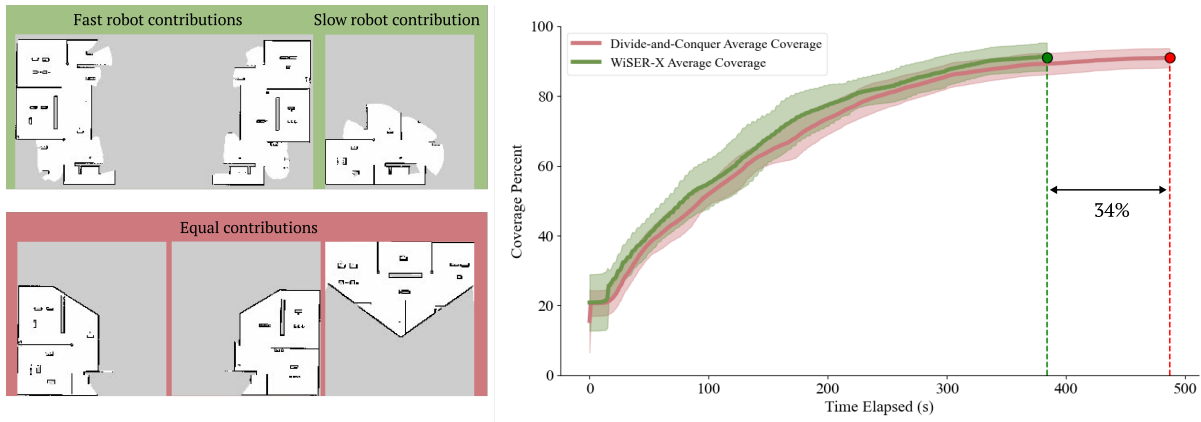


Fig. 5: Simulation results showing map coverage over time for WiSER-X and Divide-and-Conquer Baseline-3 for one slow moving robot to emulate heterogeneous behavior resulting from challenging navigation. WiSER-X reduces average termination time by 140 seconds (34%) while maintaining the same total coverage of the environment.

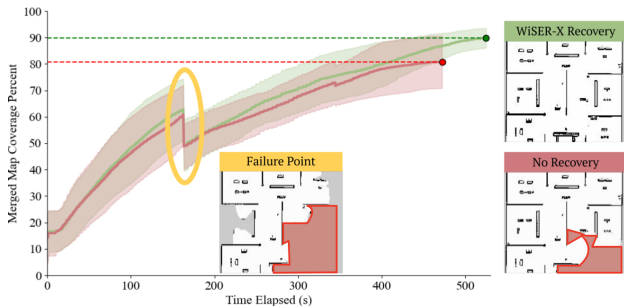


Fig. 6: An instance of simulation showing map coverage at termination time with for WiSER-X after a randomly chosen robot fails (loss of all map data from that robot, indicated in red in the images). After incorporating recovery behavior, WiSER-X enables other robots in the team to remap the area, whereas the baseline is not able to recover the lost area at termination.

and AOA measurements to determine noise’s effect on exploration termination time.

C. Experimental results for Coverage overlap and termination time

1) *Coverage overlap:* As illustrated in Fig. 3 (top), in the large simulated environment, WiSER-X leveraged only local relative position estimates, generated using groundtruth positions with added zero mean Gaussian noise and stdev of 10 cm for range measurements, 5 degrees for AOA measurements. It reduced mean coverage overlap at the end of exploration by 58% compared to the zero-information-sharing Baseline-1. Without using any additional shared information, WiSER-X resulted in only 23% more overlap than full-information-sharing Baseline-2.

We observed similar behavior for real hardware experiments where WiSER-X showed 16% lower coverage overlap in comparison to Baseline-1 and only 6% higher than Baseline-2.

2) *Termination time:* Figure 3 (bottom) shows that WiSER-X terminated, on average over 20 trials, 1.65X faster than Baseline-1 in simulation, saving about 34% time. In hardware, WiSER-X terminated 1.43X faster than Baseline-1 on average, saving 22% time. Both algorithms terminate

after Baseline-2 (on average, WiSER-X took 22% longer in simulation and 14% in hardware than Baseline-2).

Fig. 4 illustrates WiSER-X termination over 20 trials. The graph shows that while there existed an occasional outlier over the series of the explorations, the system was able to self-terminate, on average, at 93% total map coverage (3.6% standard deviation) in approximately 365 seconds (77.5 second standard deviation).

D. Simulation results for heterogeneity in robot behavior

For the scenario with variability in mapping speed, one of the three robots moved slower than the others, which reduced its overall coverage and increased the total exploration time. WiSER-X automatically addressed this issue by directing the faster robots to cover more area, compensating for the reduced performance of the slow robot. Our algorithm demonstrated a significant improvement, reducing the average termination time over 20 trials by a mean of 140 seconds (with a standard deviation of 9 seconds), or 34%, compared to Baseline-3 over aggregated runs in simulation.

The second scenario simulated complete failure of a robot, resulting in the loss of access to its local map for the area it had covered. In each of the 20 trials, one robot was randomly selected to fail after the total exploration, combining the coverage of all robots, reached between 50% and 70% completion. This timing allowed for a clear observation of the re-mapping behavior initiated by the WiSER-X algorithm compared to the baseline, without the results being influenced by the natural overlap and routing of robots in a scenario without failures. In this failure scenario, WiSER-X successfully recovered approximately 10%, (with a 4.25% standard deviation across 20 trials), of the map that otherwise would have been lost due to a robot failure. WiSER-X’s implicit coordination allowed for dynamic adaptation to robot failures and reallocation of exploration tasks in real time. Fig. 5 and Fig. 6 show the results for the two scenarios.

E. Simulation results for varying sensor noise

Wireless signal-based sensors have less than 10cm mean error in ranging and 5 degree mean error in AOA [49],

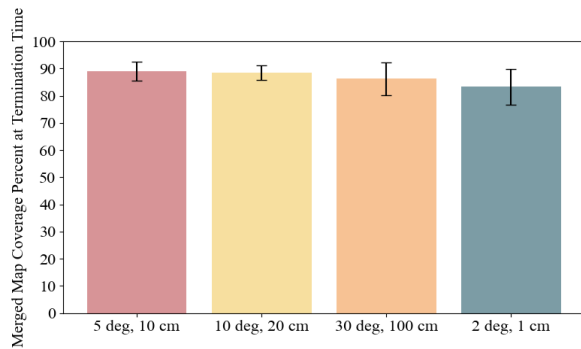


Fig. 7: Average map coverage percentage at WiSER-X termination with varying levels of sensor noise.

[51]. Hence, we add Gaussian noise into raw range and AOA measurements for each robot, simulating the following four levels of noise (in the format: AOA error & range error): 2 degrees & 1 cm, 5 degrees & 10cm, 10 degrees & 20cm, 30 degrees & 100 cm. We observed the termination time for each of these error ranges to evaluate how noise affects the system’s ability to accurately estimate total coverage and thus trigger termination.

Fig. 7 shows the relationship between varying levels in sensor measurement and the merged map coverage percent at termination time. The results show that despite increasing levels in raw noise, the system maintained a high level of map coverage at termination. This can be explained by the use of EKF localization module which allows for robust tracking despite noise in sensors. The scenario with the lowest noise did not yield the highest coverage at termination, suggesting that moderate levels of noise do not significantly impact termination in either direction (neither too much noise nor too little noise affects termination).

VI. CONCLUSION

This paper shows that sensing over wireless signals can enable the emergence of global coordination behaviors from local onboard algorithms without explicit information exchange. By extracting information directly from the transmitted wireless signals, robots can obtain relative position information without exchanging any additional information such as maps. This enables efficient multi-robot exploration in communication bandwidth limited environments where robots need only their local information to achieve coordination. Future work will explore applicability of this method with intermittent communication, underwater exploration using acoustic signals, and broader exploration scenarios where an inaccurate prior map, such as floor plan might be available.

REFERENCES

- [1] B. Yamauchi, “Frontier-based exploration using multiple robots,” in *AGENTS ’98*, 1998.
- [2] K. M. Wurm, C. Stachniss, and W. Burgard, “Coordinated multi-robot exploration using a segmentation of the environment,” *2008 IEEE/RSJ International Conference on Intelligent Robots and Systems*, pp. 1160–1165, 2008. [Online]. Available: <https://api.semanticscholar.org/CorpusID:11485678>
- [3] D. VIELFAURE, S. ARSENAULT, P. LAJOIE, and G. BELTRAME, “DORA: distributed online risk-aware explorer,” *CoRR*, vol. abs/2109.14551, 2021. [Online]. Available: <https://arxiv.org/abs/2109.14551>
- [4] S. Choudhary, L. Carlone, C. Nieto-Granda, J. G. Rogers, H. I. Christensen, and F. Dellaert, “Distributed mapping with privacy and communication constraints: Lightweight algorithms and object-based models,” *The International Journal of Robotics Research*, vol. 36, pp. 1286 – 1311, 2017.
- [5] S. Kemna and G. S. Sukhatme, “Surfacing strategies for multi-robot adaptive informative sampling with a surface-based data hub,” *OCEANS 2018 MTS/IEEE Charleston*, pp. 1–10, 2018. [Online]. Available: <https://api.semanticscholar.org/CorpusID:51986803>
- [6] R. Diamant, H. P. Tan, and L. H.-J. Lampe, “Los and nlos classification for underwater acoustic localization,” *IEEE Transactions on Mobile Computing*, vol. 13, pp. 311–323, 2014. [Online]. Available: <https://api.semanticscholar.org/CorpusID:1306551>
- [7] B. Yamauchi, “A frontier-based approach for autonomous exploration,” *Proceedings 1997 IEEE International Symposium on Computational Intelligence in Robotics and Automation CIRA’97. Towards New Computational Principles for Robotics and Automation’*, pp. 146–151, 1997.
- [8] M. Corah and N. Michael, “Distributed matroid-constrained submodular maximization for multi-robot exploration: theory and practice,” *Autonomous Robots*, vol. 43, no. 2, pp. 485–501, 2019.
- [9] M. Dharmadhikari, T. Dang, L. Solanka, J. Loje, H. Nguyen, N. Khedekar, and K. Alexis, “Motion primitives-based path planning for fast and agile exploration using aerial robots,” in *2020 IEEE International Conference on Robotics and Automation (ICRA)*, 2020, pp. 179–185.
- [10] E. Sumer and H. Temeltas, “Rrt based frontier point detection for 2d autonomous exploration,” in *2022 7th International Conference on Robotics and Automation Engineering (ICRAE)*, 2022, pp. 305–311.
- [11] K. Johansson, U. Rosolia, W. Ubellacker, A. Singletary, and A. D. Ames, “Mixed observable RRT: multi-agent mission-planning in partially observable environments,” *CoRR*, vol. abs/2110.01002, 2021. [Online]. Available: <https://arxiv.org/abs/2110.01002>
- [12] L. Schmid, M. Pantic, R. Khanna, L. Ott, R. Siegwart, and J. Nieto, “An efficient sampling-based method for online informative path planning in unknown environments,” *IEEE Robotics and Automation Letters*, vol. 5, no. 2, pp. 1500–1507, 2020.
- [13] Y. Tao, Y. Wu, B. Li, F. Cladera, A. Zhou, D. Thakur, and V. Kumar, “Seer: Safe efficient exploration for aerial robots using learning to predict information gain,” in *2023 IEEE International Conference on Robotics and Automation (ICRA)*, 2023, pp. 1235–1241.
- [14] D. Chen, A. Xiao, M. Zou, W. Chi, J. Wang, and L. Sun, “Gvd-exploration: An efficient autonomous robot exploration framework based on fast generalized voronoi diagram extraction,” 2023. [Online]. Available: <https://arxiv.org/abs/2309.06041>
- [15] D. Fox, J. Ko, K. Konolige, B. Limketkai, D. Schulz, and B. Stewart, “Distributed multirobot exploration and mapping,” *Proceedings of the IEEE*, vol. 94, no. 7, pp. 1325–1339, 2006.
- [16] E. Psomiadis, D. Maity, and P. Tsiotras, “Communication-aware map compression for online path-planning,” 2023. [Online]. Available: <https://arxiv.org/abs/2309.13451>
- [17] Z. Zhang, J. Yu, J. Tang, Y. Xu, and Y. Wang, “Mr-topomap: Multi-robot exploration based on topological map in communication restricted environment,” *IEEE Robotics and Automation Letters*, vol. 7, no. 4, pp. 10 794–10 801, 2022.
- [18] Y. Wu, Q. Gu, J. Yu, G. Ge, J. Wang, Q. Liao, C. Zhang, and Y. Wang, “Mr-gmmexplore: Multi-robot exploration system in unknown environments based on gaussian mixture model,” in *2022 IEEE International Conference on Robotics and Biomimetics (ROBIO)*, 2022, pp. 1198–1203.
- [19] V. Unhelkar and J. Shah, “Contact: Deciding to communicate during time-critical collaborative tasks in unknown, deterministic domains,” *Proceedings of the AAAI Conference on Artificial Intelligence*, vol. 30, no. 1, Mar. 2016. [Online]. Available: <https://ojs.aaai.org/index.php/AAAI/article/view/10123>
- [20] M. Kulkarni, M. Dharmadhikari, M. Tranzatto, S. Zimmermann, V. Reijgwart, P. De Petris, H. Nguyen, N. Khedekar, C. Papachristos, L. Ott, R. Siegwart, M. Hutter, and K. Alexis, “Autonomous teamed exploration of subterranean environments using legged and aerial robots,” in *2022 International Conference on Robotics and Automation (ICRA)*, 2022, pp. 3306–3313.
- [21] F. Cladera, Z. Ravichandran, I. D. Miller, M. A. Hsieh, C. J. Taylor, and V. Kumar, “Enabling large-scale heterogeneous collaboration with opportunistic communications,” 2023. [Online]. Available: <https://arxiv.org/abs/2309.15975>
- [22] H. Jiang, Y. Chang, L. Yang, X. Liu, and Y. He, “Cooperative exploration of heterogeneous uavs in mountainous environments by

- constructing steady communication,” *IEEE Robotics and Automation Letters*, vol. 8, no. 11, pp. 7249–7256, 2023.
- [23] Y. Gao, Y. Wang, X. Zhong, T. Yang, M. Wang, Z. Xu, Y. Wang, Y. Lin, C. Xu, and F. Gao, “Meeting-merging-mission: A multi-robot coordinate framework for large-scale communication-limited exploration,” in *2022 IEEE/RSJ International Conference on Intelligent Robots and Systems (IROS)*, 2022, pp. 13 700–13 707.
- [24] X. Yu and M. A. Hsieh, “Synthesis of a time-varying communication network by robot teams with information propagation guarantees,” *IEEE Robotics and Automation Letters*, vol. 5, no. 2, pp. 1413–1420, 2020.
- [25] A. R. da Silva, L. Chaimowicz, T. C. Silva, and A. Hsieh, “Communication-constrained multi-robot exploration with intermittent rendezvous,” 2024. [Online]. Available: <https://arxiv.org/abs/2309.13494>
- [26] L. Bramblett, S. Gao, and N. Bezzo, “Epistemic prediction and planning with implicit coordination for multi-robot teams in communication restricted environments,” in *2023 IEEE International Conference on Robotics and Automation (ICRA)*, 2023, pp. 5744–5750.
- [27] J. Butzke and M. Likhachev, “Planning for multi-robot exploration with multiple objective utility functions,” in *2011 IEEE/RSJ International Conference on Intelligent Robots and Systems*, 2011, pp. 3254–3259.
- [28] L. Clark, J. Galante, B. Krishnamachari, and K. Psounis, “A queue-stabilizing framework for networked multi-robot exploration,” *IEEE Robotics and Automation Letters*, vol. 6, no. 2, pp. 2091–2098, 2021.
- [29] A. Smith and G. Hollinger, “Distributed inference-based multi-robot exploration,” *Autonomous Robots*, vol. 42, pp. 1651–1668, 2018.
- [30] N. Saeed, A. Celik, T. Y. Al-Naffouri, and M.-S. Alouini, “Underwater optical wireless communications, networking, and localization: A survey,” 2018. [Online]. Available: <https://arxiv.org/abs/1803.02442>
- [31] M. Catellani and L. Sabattini, “Distributed control of a limited angular field-of-view multi-robot system in communication-denied scenarios: A probabilistic approach,” *IEEE Robotics and Automation Letters*, vol. 9, no. 1, pp. 739–746, January 2024.
- [32] Z. Xun, J. Huang, Z. Li, Z. Ying, Y. Wang, C. Xu, F. Gao, and Y. Cao, “Crepes: Cooperative relative pose estimation system,” in *2023 IEEE/RSJ International Conference on Intelligent Robots and Systems (IROS)*, 2023, pp. 5274–5281.
- [33] V. Walter, M. Saska, and A. Franchi, “Fast mutual relative localization of uavs using ultraviolet led markers,” in *2018 International Conference on Unmanned Aircraft Systems (ICUAS)*, 2018, pp. 1217–1226.
- [34] Y. Tian, K. Liu, K. Ok, L. Tran, D. Allen, N. Roy, and J. P. How, “Search and rescue under the forest canopy using multiple uavs,” *The International Journal of Robotics Research*, vol. 39, pp. 1201 – 1221, 2020.
- [35] N. Fung, J. G. Rogers, C. Nieto, H. I. Christensen, S. Kemna, and G. S. Sukhatme, “Coordinating multi-robot systems through environment partitioning for adaptive informative sampling,” *2019 International Conference on Robotics and Automation (ICRA)*, pp. 3231–3237, 2019. [Online]. Available: <https://api.semanticscholar.org/CorpusID:199542490>
- [36] S. Mayya, D. S. D’antonio, D. Saldaña, and V. Kumar, “Resilient task allocation in heterogeneous multi-robot systems,” *IEEE Robotics and Automation Letters*, vol. 6, no. 2, pp. 1327–1334, 2021.
- [37] A. A. Tziola and S. G. Loizou, “Autonomous task planning for heterogeneous multi-agent systems,” in *2023 IEEE International Conference on Robotics and Automation (ICRA)*, 2023, pp. 3490–3496.
- [38] L. Bramblett, S. Gao, and N. Bezzo, “Epistemic prediction and planning with implicit coordination for multi-robot teams in communication restricted environments,” in *2023 IEEE International Conference on Robotics and Automation (ICRA)*, 2023, pp. 5744–5750.
- [39] L. Yan, T. Stouraitis, and S. Vijayakumar, “Decentralized ability-aware adaptive control for multi-robot collaborative manipulation,” *IEEE Robotics and Automation Letters*, vol. 6, no. 2, pp. 2311–2318, 2021.
- [40] M. Coffey and A. Pierson, “Covering dynamic demand with multi-resource heterogeneous teams,” in *2023 IEEE/RSJ International Conference on Intelligent Robots and Systems (IROS)*, 2023, pp. 11 127–11 134.
- [41] N. Jadhav, W. Wang, D. Zhang, S. Kumar, and S. Gil, “Toolbox release: A wifi-based relative bearing sensor for robotics,” *International Conference on Intelligent Robots and Systems*, 2022.
- [42] N. Jadhav*, W. Wang*, D. Zhang, O. Khatib, S. Kumar, and S. Gil, “A wireless signal-based sensing framework for robotics,” *The International Journal of Robotics Research*, 2022.
- [43] S. Gil, S. Kumar, M. Mazumder, D. Katabi, and D. Rus, “Guaranteeing spoof-resilient multi-robot networks,” in *Proceedings of Robotics: Science and Systems*, Rome, Italy, July 2015.
- [44] S. Gil, S. Kumar, D. Katabi, and D. Rus, “Adaptive communication in multi-robot systems using directionality of signal strength,” *The International Journal of Robotics Research*, vol. 34, pp. 946–968, 2015.
- [45] Y. Xianjia, L. Qingqing, J. P. Queralta, J. Heikkonen, and T. Westerlund, “Applications of uwb networks and positioning to autonomous robots and industrial systems,” in *2021 10th Mediterranean Conference on Embedded Computing (MECO)*. IEEE, Jun. 2021. [Online]. Available: <http://dx.doi.org/10.1109/MECO52532.2021.9460266>
- [46] A. Arun, R. S. Ayyalasomayajula, W. Hunter, and D. Bharadia, “P2slam: Bearing based wifi slam for indoor robots,” *IEEE Robotics and Automation Letters*, vol. PP, pp. 1–1, 2022. [Online]. Available: <https://api.semanticscholar.org/CorpusID:246325404>
- [47] W. Wang, V. Cai, and S. Gil, “Mulan-wc: Multi-robot localization uncertainty-aware active nerf with wireless coordination,” *ArXiv*, vol. abs/2403.13348, 2024. [Online]. Available: <https://api.semanticscholar.org/CorpusID:268537398>
- [48] M. Cavorsi, N. Jadhav, D. Saldaña, and S. Gil, “Adaptive malicious robot detection in dynamic topologies,” *2022 IEEE 61st Conference on Decision and Control (CDC)*, pp. 2236–2243, 2022. [Online]. Available: <https://api.semanticscholar.org/CorpusID:255597504>
- [49] W. Wang, N. Jadhav, P. Vohs, N. Hughes, M. Mazumder, and S. Gil, “Active rendezvous for multi-robot pose graph optimization using sensing over wi-fi,” *International Symposium on Robotics Research*, 2019.
- [50] N. Jadhav*, S. Bhattacharya*, D. Vogt, Y. Aluma, P. Tonessen, A. Prabhakara, S. Kumar, S. Gero, R. J. Wood, and S. Gil, “Reinforcement learning–based framework for whale rendezvous via autonomous sensing robots,” *Science Robotics*, vol. 9, no. 95, p. eadn7299, 2024. [Online]. Available: <https://www.science.org/doi/abs/10.1126/scirobotics.adn7299>
- [51] A. Fishberg, B. J. Quiter, and J. P. How, “Murp: Multi-agent ultra-wideband relative pose estimation with constrained communications in 3d environments,” *IEEE Robotics and Automation Letters*, vol. 9, no. 11, pp. 10612–10619, 2024.
- [52] M. A. Shalaby, C. C. Cossette, J. Le Ny, and J. R. Forbes, “Multi-robot relative pose estimation and imu preintegration using passive uwb transceivers,” *Trans. Rob.*, vol. 40, p. 2410–2429, Feb. 2024. [Online]. Available: <https://doi.org/10.1109/TRO.2024.3370027>
- [53] W. Wang, A. Kemmeren, D. Son, J. Alonso-Mora, and S. Gil, “Wi-closure: Reliable and efficient search of inter-robot loop closures using wireless sensing,” *2023 IEEE International Conference on Robotics and Automation (ICRA)*, pp. 2069–2075, 2022. [Online]. Available: <https://api.semanticscholar.org/CorpusID:252693169>
- [54] J. Banfi, A. Q. Li, I. M. Rekleitis, F. Amigoni, and N. Basilico, “Strategies for coordinated multirobot exploration with recurrent connectivity constraints,” *Autonomous Robots*, vol. 42, pp. 875–894, 2018.
- [55] B. Zhou, Y. Zhang, X. Chen, and S. Shen, “Fuel: Fast uav exploration using incremental frontier structure and hierarchical planning,” *IEEE Robotics and Automation Letters*, vol. 6, pp. 779–786, 2020. [Online]. Available: <https://api.semanticscholar.org/CorpusID:225041227>
- [56] O. Peltzer, A. Bouman, S.-K. Kim, R. Senanayake, J. Ott, H. Delecki, M. Sobue, M. J. Kochenderfer, M. Schwager, J. Burdick, and A.-a. Agha-mohammadi, “Fig-op: Exploring large-scale unknown environments on a fixed time budget,” in *2022 IEEE/RSJ International Conference on Intelligent Robots and Systems (IROS)*, 2022, pp. 8754–8761.
- [57] S. Kumar, S. Gil, D. Katabi, and D. Rus, “Accurate indoor localization with zero start-up cost,” in *Proceedings of the 20th annual international conference on Mobile computing and networking*, 2014.
- [58] J. Xiong and K. Jamieson, “Arraytrack: A fine-grained indoor location system,” in *Proceedings of the 10th USENIX Conference on Networked Systems Design and Implementation*, ser. nsdi’13, 2013, p. 71–84.
- [59] J. Hörner, “Map-merging for multi-robot system.” [Online]. Available: <https://github.com/hrnr/m-explore>
- [60] H. Umari and S. Mukhopadhyay, “Autonomous robotic exploration based on multiple rapidly-exploring randomized trees,” in *2017 IEEE/RSJ International Conference on Intelligent Robots and Systems (IROS)*, Sept 2017, pp. 1396–1402.
- [61] S. M. LaValle, “Rapidly-exploring random trees : a new tool for path planning,” *The annual research report*, 1998. [Online]. Available: <https://api.semanticscholar.org/CorpusID:14744621>
- [62] G. Grisetti, C. Stachniss, and W. Burgard, “Improved techniques for

grid mapping with rao-blackwellized particle filters," *IEEE Transactions on Robotics*, vol. 23, no. 1, pp. 34–46, 2007.